Awe *et al. Appl Biol Chem* (2020) 63:12
https://doi.org/10.1186/s13765-020-00494-1

KSABC
The Korean Society for Applied Biological Chemistry

ARTICLE Open Access

Preparation and characterisation of activated carbon from *Vitis vinifera* leaf litter and its adsorption performance for aqueous phenanthrene

Adetunji Ajibola Awe[1*], Beatrice Olutoyin Opeolu[2], Olalekan Siyanbola Fatoki[3], Olushola Sunday Ayanda[4], Vanessa Angela Jackson[5] and Reinette Snyman[6]

Abstract

The adsorption of phenanthrene onto activated carbons produced from *Vitis vinifera* leaf litter (a waste plant biomass) was investigated in this study. Zinc chloride ($ZnCl_2$) and phosphoric acid (H_3PO_4) were utilised as activating agents in producing the activated carbons. The characterisation of the activated carbons was achieved with Fourier transform infrared spectroscopy (for surface functional groups), scanning electron microscopy (for surface morphology) and Brunauer–Emmett–Teller (BET) (for surface area determination). The adsorption of phenanthrene onto the activated carbons was optimised in terms of solution pH, adsorbent dosage, initial concentration of adsorbate solution and contact time. Experimental results showed that H_3PO_4 modified activated carbon gave better yield (up to 58.40%) relative to $ZnCl_2$ modified activated carbon (only up to 47.08%). Meanwhile, surface characterisation showed that $ZnCl_2$ modification resulted in higher BET surface area (up to 616.60 m^2/g) and total pore volume (up to 0.289 cm^3/g) relative to BET surface area of up to 295.49 m^2/g and total pore volume of up to 0.185 cm^3/g obtained from H_3PO_4 modified activated carbons. Adsorption equilibrium data fitted well into Freundlich isotherm model relative to other applied isotherm models, with maximum K_f value of 1.27 for $ZnCl_2$ modified activated carbon and 1.16 K_f value for H_3PO_4 modified activated carbon. The maximum adsorption capacity for $ZnCl_2$ and H_3PO_4 activated carbons for the removal of phenanthrene were 94.12 and 89.13 mg/g, respectively. Kinetic studies revealed that dynamic equilibrium was reached at 80 min contact time. Experimental data fitted best into the Elovich kinetic model relative to other kinetic models, based on the correlation coefficient (R^2) values obtained from kinetic studies. Chemisorption was deduced as a major phenanthrene removal pathway from aqueous solution and the physicochemical characteristics of the adsorbents have major influence on phenanthrene removal efficiencies.

Keywords: Phenanthrene, Adsorption, Activated carbon, *Vitis vinifera*, Biomass

Introduction

Contamination of the aquatic system poses a serious threat to the aquatic organisms and human health. The occurrence of environmental contaminants such as polycyclic aromatic hydrocarbons (PAHs) could possibly lead to loss of biodiversity, environmental degradation, significant adverse health effects, hunger and poverty amongst other impacts [1–3]. The lipophilic nature of PAHs have resulted in their bioaccumulation in aquatic organisms and are very dangerous in terms of potential impacts on sufficiently exposed aquatic organisms [1]. Phenanthrene is one of the 16 priority PAHs that is found frequently in various environmental matrices and

*Correspondence: tunjyaweson2007@gmail.com
[1] Department of Chemistry, Cape Peninsula University of Technology, Cape Town, South Africa
Full list of author information is available at the end of the article

has been reported to be toxic to aquatic organisms even while present at low concentrations [4].

Hence, the removal of organic contaminants such as phenanthrene from wastewaters is of immense importance. A wide range of treatment technology has been explored in the past for possible remediation of wastewaters. These includes; adsorption, precipitation, coagulation-flocculation, sedimentation, flotation, filtration, membrane processes, electrochemical techniques, biological processes, chemical reactions and ion exchange amongst others [5–7]. In recent times, adsorption treatment technology, which is a surface phenomenon had been recognised as the most efficient and promising approach in wastewater treatment, due to its simplicity, economic viability, technical feasibility, insensitivity to toxicants, high removal capacity for wide-range of pollutants and environmental friendliness [5, 8]. Meanwhile, adsorption technique has its own limitations; such as non-destructive nature of the pollutant which could lead to secondary pollution, challenges of regeneration and post treatment of adsorbents.

Several adsorbents have been utilised in the removal of environmental contaminants from wastewaters. Amongst which, activated carbons have attracted enormous research interest due to their high internal surface area, microporosity, contaminant removal efficiency, chemical nature, and environmental friendliness [9, 10]. Agricultural wastes biomass, which contains hemicellulose, lignin, extractives, lipids, proteins, simple sugars, hydrocarbon forms, and starch (with functional groups that facilitate adsorption) have served as precursors for the production of low-cost and high adsorption capacity activated carbons [9, 10]. Lignin in agricultural biomass is thought to be a major component that adsorbs organic pollutants like PAHs from aqueous solution [11].

Plant residues are often preferred over living biomass, because they are not affected by toxic wastes, do not require nutrients, and can often be regenerated and reused for many treatment cycles. Dead biomass may also be used or stored for extended periods at room temperature without putrefaction occurring [12]. Plant residues, wood chips, ryegrass root, orange peels, bamboo leaves and pine needles were studied by Chen et al. [13] for their capacity to adsorb PAHs in batch biosorption experiments. Phenanthrene sorption coefficients reported, ranged from 2484 to 5306 L/kg and the lowest was for wood chips, which has low vibration band intensity for lignin and high sugar content (60.6%). The results showed that plant residues with high lignin content have enormous potential for removing PAHs and suggested that lowering the polar components (mainly sugar) of plant derived biosorbents could enhance sorption capability. Modified pine bark (through acid hydrolysis) with increased lignin content has also been reported to display enhanced phenanthrene-sorption (from 62.91 up to 91.16% PAH-removal) compared to the raw pine bark that has low lignin content [14]. Lignin was assumed to be the main sorption medium in pine bark for organic pollutants due to its hydrophobic nature.

Biomass from *Vitis vinifera* (*V. vinifera*) also known as grape have also been studied for their adsorption potential; grape peel for dye-sorption [15] and grape waste from wine production for Cr (VI)-sorption [16]. Chand et al. [16] reported that Cr (VI) was selectively adsorbed over other metal ions tested by cross-linked grape waste gel. The adsorption of Cr (VI) was reported to be highly dependent on pH, with maximum adsorption (1.91 mol/kg) at pH 4. Their study established the potential of grape waste as an effective adsorbent. Saeed et al. [15] reported the sorption of crystal violet dye by grape fruit peel. The study demonstrated that grape fruit peel could be used as a cost-effective adsorbent for the removal of crystal violet dye from aqueous solution. Crystal violet removal was reported to be dependent upon process parameters such as pH, sorbate and sorbent concentration, and contact time as shown by batch adsorption studies.

Vitis vinifera were first cultivated in Mediterranean countries over thousands of years ago, [17]. The cultivation of *V. vinifera* is now common all over the world, surface covered with vineyards amounted to almost eight million hectares worldwide, as at 2008 and often represents a very profitable endeavour [17]. The total harvest of *V. vinifera* worldwide is about 60 million metric tons per year and about 80% of the harvest being utilised in wineries [18]. In South Africa, 101,259 hectares (ha) of land are used for grape wine cultivation, which places South Africa at 14th place in terms of hectares used for wine grape production and the 7th largest producer of wine in the world [19]. Consequently, wastes from wineries could serve as precursors for agricultural based activated carbons. This provides an opportunity to explore the possible utilisation of this resource for the abatement of recalcitrant PAHs, in a way that will provide environmental and economic benefits, as well as reducing the problems associated with their disposal. This informed the production of activated carbons from agro-wastes for PAHs removal from aqueous solution.

The non-polar nature of phenanthrene hinders its bioavailability and biodegradation rates, making biosorption a more suitable remediation approach for phenanthrene. Biosorption avoids the generation of toxic sludge and can be used under a broad range of operating conditions such as pH, adsorbate concentration and temperature, amongst others [20]. Sorption of contaminant such as heavy metals, dyes, pesticides and organic pollutants have been reported in literature [12, 21, 22]. Therefore,

the objective of this research is to investigate the capacity of activated carbons prepared from *V. vinifera* leaf litter for the removal of phenanthrene from aqueous solutions.

Materials and methods

Chemicals

The phenanthrene ($C_{14}H_{10}$) standard was purchased from Supelco, Bellefonte, PA, USA. Separations (South Africa) supplied the GHP acrodisc syringe filters and amber glass vials with Teflon lined screw caps. Phosphoric acid (H_3PO_4), zinc chloride ($ZnCl_2$), acetonitrile and all other chemicals were obtained from Sigma Aldrich (South Africa). Milli-Q water from Merck Millipore (USA) Milli-Q synthesis system was used for all analytical preparations.

Collection and analysis of *V. vinifera* leaf litter

Dried *V. vinifera* leaf litter, an agricultural waste was collected at Stellenbosch, Western Cape, South Africa, into a precleaned sack. It was transported to the laboratory and stored in a cool dry place until further processing. The suitability of *V. vinifera* leaf litter as precursor for activated carbons was assessed by the determination of moisture, ash and crude fibre contents. The elemental composition of the milled *V. vinifera* leaf litter was obtained through Energy-dispersive X-ray spectroscopy (EDS).

Carbonisation

The carbonisation method was based on that reported by Sudaryanto et al. [23]. The leaf litter was milled and sieved with a standard mesh to obtain a particle size of ≤ 25 mesh (≤ 707 µm). The sieved milled leaf litter was impregnated with the activating agent (H_3PO_4 and $ZnCl_2$) at 5:2, 5:1 and 10:1 biomass to activating agent ratios, respectively. The slurry after impregnation was sonicated at 50 °C for 3 h before drying at 110 °C overnight. 20 g of the impregnated biomass was carbonised at 600 °C for 1 h and N_2 flow of 150 mL/min. The carboniser was switched off and allowed to cool to 200 °C with the nitrogen gas still flowing. The gas supply was cut off at 200 °C, the activated carbon obtained was placed in a desiccator to cool. The charred biomass was subsequently weighed and percentage yield (Eq. 1), burn off (Eq. 2) and attrition (Eq. 3) calculated. The carbonised biomass was washed with hot 1 M HCl, followed by milli-Q water until all acid was removed, and further dried at 50 °C for 5 h.

$$\%Yield = \frac{M_1}{M_2} \times 100\% \quad (1)$$

$$\%Burn\ off = \left(100 - \%yield\right) \quad (2)$$

$$\%Attrition = \frac{A - B}{A} \times 100\% \quad (3)$$

where M_1 is the mass of charred biomass, M_2 is the mass of uncharred biomass, A is the Initial weight of charred biomass before washing with hot 1 M HCl and milli-Q water and B is the Final weight of charred biomass after washing with hot 1 M HCl and milli-Q water.

Characterisation of activated carbon

Fourier transform infrared spectrometry

The Fourier transform infrared (FTIR) spectra of the activated carbons and raw *V. vinifera* leaf litter (recorded over 4000–400 cm^{-1} range) were obtained on a Universal Attenuated Total Reflectance (UATR) Infrared spectrometer Perkin Elmer Spectrum 2 (UK). The crystal area of the instrument was cleaned prior to analysis and background correction made. The samples were placed directly on the crystal area of the universal diamond attenuated total reflectance (ATR) top-plate. The pressure arm was positioned over the crystal-sample area, then locked into a precise position above the diamond crystal and force applied to the sample, pushing it onto the diamond surface. The sample was scanned to obtain the spectrum.

Scanning electron microscopic analysis

The surface morphologies of the adsorbents were obtained, using scanning electron microscope (Nova Nano SEM 230, USA). A gold sputtering device (JOEL, JFC-1600) was utilised in coating the samples with a fine layer of gold for clarity to obtain the surface morphology. The elemental contents of activated carbons were also obtained by EDS [24].

Brunauer–Emmett–Teller

An automatic adsorption instrument (Quanta chrome Corp. Nova-1000 g gas sorption, USA) was utilised in obtaining the textural properties of the activated carbons. The Brunauer–Emmett–Teller (BET) surface area, total pore volume, micropore area, micropore volume and pore size were obtained. Degassing of samples was carried out at 170 °C for 13 h, before the adsorption and desorption of liquid N_2 at 77 K. MicroActive 4.00 software (TriStar II 3020 version 2.00) was utilised to generate the BET surface area and the BJH (Barrett, Joyner and Helenda) pore distribution of the activated carbons.

Adsorption studies

Adsorption studies were carried out using phenanthrene as the adsorbate. Phenanthrene is one of the

most abundant PAHs and an acceptable representative of semi volatile organic compounds [25, 26]. Due to the poor solubility of phenanthrene in water, milli-Q water containing 30% acetonitrile was utilised for this study. Parameters such as contact time, adsorbent load, pH and initial concentration were investigated to establish the optimum values for adsorbents efficiencies. The obtained data was fitted into adsorption kinetic models and isotherms to evaluate the quality of the adsorbents and to describe the mechanism of the sorption process.

Effect of pH

To investigate the effect of pH, 25 mL of 1 mg/L phenanthrene solutions with varying pH values (3–12) and 0.1 g activated carbon was utilised. The desired pH of the 0.1 mg/L phenanthrene solution was prepared from 10 mg/L solution with the addition of either 0.1 M HCl or 0.1 M NaOH to adjust the pH as required for obtaining the pH values of 3, 6, 9 and 12 investigated. A 25 mL phenanthrene solution that has been adjusted to the required pH was added to 0.1 g activated carbon in a 50-mL amber bottle and covered with Teflon-lined lid. This was thereafter placed on an orbital shaker at 298 K and allowed for 180 min at 100 revolutions per minute (rpm). After which 1 mL was filtered through a GHP acrodisc syringe filter (0.2 µm, 13 mm), prior to GC-FID analysis for the quantification of the residual phenanthrene.

Effect of adsorbent dosage

The effect of adsorbent dosage was studied using 25 mL of 1 mg/L phenanthrene solution at pH 3 with varying weights (0.01–0.1 g) of adsorbents. The investigated weights (0.01, 0.025, 0.050, 0.075 and 0.1 g) of adsorbents were carefully weighed into 50-mL amber bottles and 25 mL of phenanthrene solution added and covered with Teflon-lined lids. The bottles and their contents were then placed on the orbital shaker at 298 K and allowed for 180 min at 100 rpm. Thereafter, 1 mL solution from each of the bottles was filtered through GHP filter and the filtrates analysed with GC-FID for the residual phenanthrene.

Effect of initial phenanthrene concentration

The effect of initial concentration was studied using 25 mL of phenanthrene solution of varying concentrations. The concentrations investigated were 1, 2, 3, 4 and 5 mg/L that have been adjusted to pH 3. Aliquot 25 mL of the phenanthrene solutions were measured into 50-mL amber bottles containing 0.1 g of adsorbents. The experiments were carried out on an orbital shaker at 298 K, 100 rpm for 180 min and the GHP filtrates analysed.

Effect of contact time

The effect of contact time on the adsorption of phenanthrene was investigated by varying the time of mixing the adsorbent and the phenanthrene solution on an orbital shaker at 298 K. Phenanthrene concentration of 1 mg/L (25 mL) that have been adjusted to pH 3 and 0.1 g of adsorbents were utilised. The time intervals investigated were 10, 20, 40, 60, 80, 120, and 180 min. Amber bottles with Teflon-lined lids were used and the GHP filtrates analysed.

Gas chromatography–flame ionisation detection (GC-FID) instrument was utilised for the determination of phenanthrene in aqueous solutions before and after adsorption experiment. The percentage of phenanthrene removal and the equilibrium adsorption capacity (q_e) were estimated using Eqs. 4 and 5, respectively.

$$\%\, Adsorbed = \frac{C_0 - C_t}{C_0} \times 100 \tag{4}$$

$$q_e = \frac{V(C_0 - C_e)}{m} \tag{5}$$

where C_0 (mg/L), C_e (mg/L) and C_t (mg/L) are initial, equilibrium and after time t concentration of phenanthrene solution, respectively, V (L) is the volume of phenanthrene solution, m (g) is the mass of adsorbent and q_e (mg/g) is the equilibrium adsorption capacity of adsorbent [26].

Adsorption isotherms

Adsorption isotherm models were used to describe adsorption behaviour of analytes onto the surface of adsorbents at equilibrium. The amount of phenanthrene adsorbed, and removal efficiency of adsorbents could be deduced from the adsorption isotherm models.

Langmuir isotherm

The sorption of phenanthrene onto single layer of selected activated carbon surface was studied with Langmuir isotherm model. Langmuir isotherm model postulates that, there is no transmigration of adsorbate in the plane of adsorbent surface for single layer adsorption onto a surface with a finite number of identical sites and uniform energies of adsorption [27]. A linearised equation for Langmuir isotherm model is given in Eq. 6.

$$\frac{1}{q_e} = \frac{1}{q_m} + \frac{1}{q_m K_L C_e} \tag{6}$$

where q_e is the amount of phenanthrene adsorbed per gram of the adsorbent at equilibrium (mg/g), q_m

represent the maximum monolayer coverage capacity (mg/g), K_L is Langmuir isotherm constant (L/mg) and C_e is the equilibrium concentration of phenanthrene (mg/L).

The separation factor or equilibrium parameter (R_L) which is the crucial feature of the Langmuir isotherm model [28] is presented as Eq. 7:

$$R_L = \frac{1}{1 + (1 + K_L C_o)} \tag{7}$$

where C_o is the initial phenanthrene concentration (mg/L).

The nature of adsorption can be adjudged from the value of R_L; $R_L > 1$ unfavourable, $R_L = 1$ linear, $0 < R_L < 1$ favourable and $R_L = 0$ irreversible [29].

Freundlich isotherm

The adsorption characteristic of phenanthrene onto heterogeneous surfaces of the produced activated carbons was investigated by Freundlich adsorption isotherm. This isotherm model, assumes that the adsorbent has a heterogenous surface with adsorption sites that have different energies of adsorption that are not always available [30]. The linearised Freundlich adsorption isotherm equation is presented as Eq. 8:

$$\log q_e = \log K_f - \frac{1}{n} \log C_e \tag{8}$$

where q_e is the amount of phenanthrene adsorbed per gram of adsorbent at equilibrium (mg/g), K_f is the Freundlich isotherm constant (mg/g), n is adsorption intensity, and C_e is the concentration of phenanthrene at equilibrium (mg/L).

The Freundlich constant n gives an indication of adsorption intensity, while K_f gives an indication of adsorption capacity. The extent of non-linearity between solution concentration and adsorption depends on n. Linear adsorption, chemical adsorption and favourable physical adsorption processes are indicated by $n = 1$, $n < 1$, and $n > 1$, respectively [31].

Temkin isotherm

Experimental data obtained were assessed with Temkin isotherm model. Indirect adsorbent/adsorbate interactions influence on adsorption isotherms could be evaluated [32]. The model ignores the extremely low and large adsorbate concentration values and assumes that the heat of adsorption of all of the molecules in the layer would decrease linearly instead of logarithmically with coverage due to adsorbate/adsorbent interactions [31]. The linear equation is expressed as Eq. 9:

$$q_e = B \ln K_T + B \ln C_e \tag{9}$$

where B (J/mol) and K_T are Temkin constants related to heat of sorption and maximum binding energy, respectively, R is the gas constant (8.31 J/mol K), and T (K) is the absolute temperature.

Dubinin–Radushkevich isotherm

Experimental data obtained were also fitted into the Dubinin–Radushkevich isotherm model, which had been widely utilised to describe adsorption onto microporous materials of carbonaceous origin [33–35]. The linear equation is expressed as Eq. 10:

$$\ln q_e = \ln (q_{DRB}) - \left(K_{ad} \varepsilon^2\right) \tag{10}$$

where q_e is the amount of phenanthrene adsorbed per gram of adsorbent at equilibrium (mg/g), q_{DRB} is the theoretical isotherm saturation capacity (mg/g), K_{ad} is the Dubinin–Radushkevich isotherm constant (mol^2/kJ^2) and ε is the Dubinin-Radushkevich isotherm constant [34].

Kinetic studies

To gain valuable information into the reaction pathways, the rate of adsorption and the mechanism of adsorption, adsorption kinetics study were carried out. These insights were needed to establish the efficiency of adsorbents and to determine the optimum operating conditions for the adsorption process [36]. Experimental data obtained were subjected to four kinetic models (pseudo-first order kinetic, pseudo-second order kinetic, Elovich and intra-particle diffusion models).

Pseudo-first order kinetic model

The pseudo-first order kinetic model, also known as Lagergren kinetic, had its adsorption rate equation (for a liquid–solid system) derived, based on the adsorbent adsorption capacity. This adsorption rate equation is commonly used for solute adsorption from liquid matrix [37].

The simplified pseudo first order kinetic equation can be expressed as Eq. 11:

$$\mathrm{In}(q_e - q_t) = \mathrm{Inq_e} - k_1 t \tag{11}$$

where q_e and q_t are the amount of solute adsorbed per unit mass of adsorbent (mg/g) at equilibrium and at time t respectively and k_1 is the rate constant.

Pseudo-second order kinetic model

The pseudo-second order model is based on the sorption capacity of the solid phase which is associated with the number of available active sites. The linearised form of the kinetic model is expressed as Eq. 12 [38].

$$\frac{t}{q_t} = \frac{1}{k_2 q_e^2} + \frac{1}{q_e}(t) \quad (12)$$

k_2 is the pseudo-second order rate constant. This model is advantageous as it eliminates the problem of assigning q_e. The kinetics is presumed to proceed via chemisorption, being the rate determining step [38].

Elovich model

The Elovich model (Eq. 13) has been widely utilised to describe chemical adsorption processes and it is applicable for systems with heterogenous adsorbing surfaces [39].

$$q_t = \left(\frac{1}{\beta}\right) ln(\alpha \cdot \beta) + \left(\frac{1}{\beta}\right) ln(t) \quad (13)$$

where q_t is the sorption capacity at time t (mg/g), α is the initial sorption rate (mg/g min), β is the desorption constant (g/mg) during any one experiment [38].

A plot of q_t versus ln(t) gives a straight-line graph with a slope of (1/β) and intercept of (1/β) ln(αβ).

Intraparticle diffusion model

To describe the adsorption of phenanthrene onto activated carbon from a mechanistic point of view, the Weber Morris intraparticle diffusion model was used. This model is based on the hypothesis that the overall adsorption process maybe controlled either by one or combinations of more than one factors. These include film or external diffusion, pore diffusion, surface diffusion and adsorption onto the adsorbent pore surface [40, 41]. The expression for the model is expressed as Eq. 14:

$$q_t = K_{id} \cdot t^{\frac{1}{2}} + C \quad (14)$$

where q_t is the amount of phenanthrene adsorbed at time t (mg/g), K_{id} is the intraparticle diffusion rate constant (mg/g $min^{1/2}$) and C (mg/g) is the constant related to the thickness of the boundary layer (the higher the value of C, the greater the boundary layer effect) [40].

Results and discussion

Characterisation

The ash, moisture, crude fibre and elemental composition of *V. vinifera* leaf litter are presented in Table 1. The ash, moisture and crude fibre content obtained were 7.22%, 8.19% and 13%, respectively. The energy dispersion spectroscopic (EDS) analysis showed that *V. vinifera* contained 52.82% carbon, 46.05% oxygen, 0.41% calcium, 0.07% sulphur and 0.64% copper. These results make *V. vinifera* leaf litter a promising precursor for activated carbon. Precursors with high carbon content but with low ash and sulphur content results in high yield activated carbon with high adsorption capabilities and low/no emission of culprit sulphur oxides during the carbonisation process [42, 43]. The results obtained from the analysis of the *V. vinifera* leaf litter, suggest that the material can be utilised as a cheap biomass in the production of activated carbon with great adsorption capabilities.

Table 1 Ash, moisture, crude fibre and atomic elements of *V. vinifera* leaf litter

Ash, moisture and crude fibre (wt%)	
Ash content	7.22
Moisture content	8.19
Crude fibre content	13.00
Elemental composition (wt%)	
Carbon	52.82
Oxygen	46.05
Calcium	0.41
Sulphur	0.07
Copper	0.64

The yield, burn-off, attrition and elemental composition of charred products using two different activated agents are presented in Table 2. The yield obtained for chars were high (41.63 to 58.40%) with the exception of inactivated char (Nac) with 32.84% yield. Improved yield was obtained for biomass activated with H_3PO_4 and $ZnCl_2$. Yield was directly proportional to the concentration of the activating agent for the range studied. The more the activating agent the less the burn-off obtained (41.98 to 67.17%). The highest burn-off was obtained for Nac char. Chemical agents have been reported to improve the yield and lower burn-off of conversion products at low concentrations. They act as catalysts to promote depolymerisation of cellulose, bond cleavage, hydrolysis, dehydration, condensation and cross-linkage with biopolymers [44, 45]. At optimum level of activating agents, activated carbon with maximum uniform micrporosity are formed [44, 45]. The observed improved yields were higher than those reported by Adebowale and Bayer [42]. Attrition ranged from 9.24 to 42.86%, with Nac char having the lowest attrition and that activated with the highest proportion of $ZnCl_2$ (ZAac) had the highest attrition (Table 2). The percentage fixed carbon ranged from 51.37 to 67.38% and followed similar trend observed for percentage yield for each activating agent. Activation with $ZnCl_2$ gave higher fixed carbon in most instances relative to H_3PO_4 activation (Table 2).

The carbon matrix is not solely made-up of carbon atoms but consists of other atoms too. Oxygen, phosphorous, silicon, calcium, chlorine, sulphur, copper and zinc were atoms detected in activated carbons that were produced. These atoms are bonded to the edges of carbon

Table 2 Yield, burn-off, attrition and elemental composition of the chars

Ratio (biomass: chemical)/ chemical agent	Name	%Yield	%Burn-off	%Attrition	Elemental composition (wt%)								
					C	O	P	Si	Ca	Cl	S	Cu	Zn
5:2/ H_3PO_4	PAac	58.40	41.98	36.75	60.04	37.64	1.04	0.14	0.51	0.04	0.03	0.56	–
5:1/ H_3PO_4	PBac	47.04	52.96	19.67	57.60	41.13	0.87	–	0.04	–	–	–	–
10:1/ H_3PO_4	PCac	41.63	58.37	16.21	57.58	40.23	0.01	0.37	0.53	0.69	–	0.58	–
5:2/ $ZnCl_2$	ZAac	47.08	52.92	42.86	67.21	30.87	–	0.00	–	0.43	0.00	1.48	–
5:1/ $ZnCl_2$	ZBac	45.54	54.46	22.67	62.38	32.16	–	0.13	0.77	2.66	0.16	–	1.74
10:1/ $ZnCl_2$	ZCac	44.65	55.36	16.00	52.21	42.86	–	0.72	0.72	1.82	0.14	0.47	0.88
No activation	Nac	32.84	67.16	9.24	51.37	45.17	1.64	0.72	0.93	0.18	–	–	–

layers and governs the surface chemistry of activated carbons [46]. Oxygen was detected in all the chars and ranged from 30.87 to 45.17%. Phosphorous was detected in H_3PO_4 treated and untreated products and ranged from 0.01 to 1.64%. However, Zn was only detected in products treated with $ZnCl_2$ and ranged from 0.86 to 1.74% (Table 2).

The textural properties of the activated carbons are presented in Table 3. The BET surface area ranged from 24.5399 to 616.6038 m^2/g. Increase in concentration of activating agent led to increased surface area. The micropore area also increased with increasing concentration of activating agent with values between 17.5864 and 462.5162 m^2/g. The micropore volume ranged between 0.0069 and 0.1843 cm^3/g while the single point adsorption total pore volume ranged between 0.021259 and 0.289066 cm^3/g. Similar trend was observed in all adsorbent properties, with the exception of pore size. The observed pore size ranged between 1.87521 nm and 4.05688 nm.

The surface area of 617 m^2/g and a pore volume of 0.3 cm^3/g showed the potential of *Vitis vinifera* leaf litter for activated carbon production. Commercially available activated carbons has surface area of about 1000 m^2/g and pore volume between 0.2 and 0.5 cm^3/g [42]. The results obtained from this study is comparable with that of Bagheri & Abedi [47]. The authors produced activated carbons with surface area ranging from 105 to 1320 m^2/g from corn cob activated with 1:2 corn/chemical ratio. They reported that biomass/chemical ratio and method of mixing i.e. mixing-filtration, solid–solid and impregnation were the most important parameters for obtaining optimal experimental conditions. The activated carbon with the highest BET surface area (1320 m^2/g) produced at the optimal experiment conditions was subsequently tested in a natural gas adsorption system. A 120 v/v natural gas adsorption capacity was reported. The importance of biomass/chemical ratio in improving the BET surface area of activated carbons can be seen clearly with the data obtained in this study (Table 3), increased from 10:1 to 5:2 biomass/chemical ratio led to increase in BET surface area of 24.54 to 616.60 m^2/g with $ZnCl_2$ activating agent.

The BET isotherms for nitrogen adsorption obtained with the activated carbons are presented in Fig. 1. The activated carbon ZAac with the highest BET surface area (616.60 m^2/g) gave the highest nitrogen adsorption capacity of 8.37 mmol/g, while the activated carbon ZCac with the lowest BET surface area (24.54 m^2/g) gave the lowest nitrogen adsorption capacity of 0.64 mmol/g.

Table 3 Textural properties of the activated carbons

Activated carbon	Surface area (m^2/g)	Micropore area (m^2/g)	Micropore volume (cm^3/g)	Total pore volume (cm^3/g)	Pore size (nm)
PAac	295.4881	174.1876	0.0720	0.185445	2.51036
PBac	171.8277	104.7176	0.0423	0.141699	3.29863
PCac	109.9583	82.1013	0.0323	0.060340	2.19501
ZAac	616.6038	462.5162	0.1843	0.289066	1.87521
ZBac	120.8772	68.9333	0.0280	0.122596	4.05688
ZCac	24.5399	17.5864	0.0069	0.021259	3.46522

PAac: activated with H_3PO_4 at 5:2 biomass to H_3PO_4 ratio. PBac: activated with H_3PO_4 at 5:1 biomass to H_3PO_4 ratio. PCac: activated with H_3PO_4 at 10:1 biomass to H_3PO_4 ratio. ZAac: activated with $ZnCl_2$ at 5:2 biomass to $ZnCl_2$ ratio. ZBac: activated with $ZnCl_2$ at 5:1 biomass to $ZnCl_2$ ratio. ZCac: activated with $ZnCl_2$ at 10:1 biomass to $ZnCl_2$ ratio

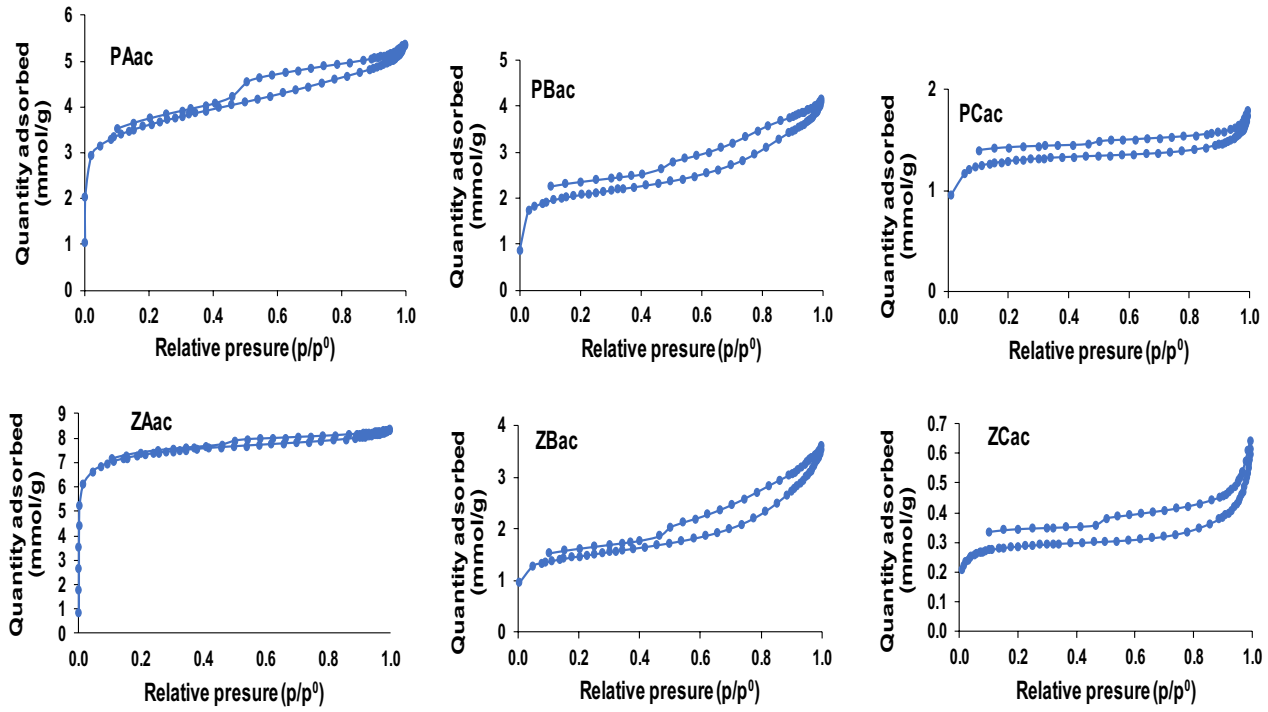

Fig. 1 BET isotherm plots for nitrogen adsorption capacity of the activated carbons PAac: activated with H_3PO_4 at 5:2 biomass to H_3PO_4 ratio. PBac: activated with H_3PO_4 at 5:1 biomass to H_3PO_4 ratio. PCac: activated with H_3PO_4 at 10:1 biomass to H_3PO_4 ratio. ZAac: activated with $ZnCl_2$ at 5:2 biomass to $ZnCl_2$ ratio. ZBac: activated with $ZnCl_2$ at 5:1 biomass to $ZnCl_2$ ratio. ZCac: activated with $ZnCl_2$ at 10:1 biomass to $ZnCl_2$ ratio

Thus, BET surface area of activated carbons plays a crucial role in their adsorption capabilities.

Chemical structure information of the biomass and charred products was obtained by infrared spectroscopy (Fig. 2). Charred products were largely similar but differed from the precursor structurally. The asymmetrical stretching vibration of C–H bond at 2918 cm^{-1} and the symmetrical stretching vibration at 2851 cm^{-1} present in the precursor were obviously absent in charred products. The C–H bonds were probably broken during the thermal conversion process to form a more stable C=C bonds, that was observed at 1580 cm^{-1} for all the charred products. Moreover, the C=O stretching observed at 1734 cm^{-1} in the raw biomass was absent in charred products, as surface oxygenated groups were converted to CO and CO_2 during thermal conversion [35, 48–50]. The bands at around 1580 cm^{-1} and 1070 cm^{-1} observed in all charred products are indicative of C=C bond stretching ascribed to aromatic compounds.

The scanning electron microscopy (SEM), a good tool for surface morphology characterisation of adsorbents [31] was also utilised for characterising the activated carbon. Figure 3 shows the SEM images of charred products and raw biomass. The SEM image of raw biomass is smooth with no evidence of porosity, while rough surfaces and evidence of porosity could be observed on the SEM images of charred products. The porosity of charred products was due to the decomposition of lignin, cellulose and hemicellulose during carbonisation, resulting in the formation of micropores and mesopores [51].

Adsorption of phenanthrene onto activated carbons

The adsorption of phenanthrene on the activated carbons was studied to determine the potential of the charred products for remediation of PAHs contaminated water. Optimisation of experimental parameters for the adsorption processes was considered.

Effect of pH

The results obtained showed that the adsorption of phenanthrene was favourable in the acidic medium relative to alkaline conditions (Fig. 4). This observation is consistent with that reported by Gupta [26], who stated that the adsorption of phenanthrene on activated carbon derived from orange peel, was maximum at low pH values and least at high pH value. The increase in positive charge on the adsorbent surface at low pH led to higher interaction between the adsorbent surface and the phenanthrene molecule (having π-electron cloud). At low pH, there will be availability of more protons to enhance electrostatic

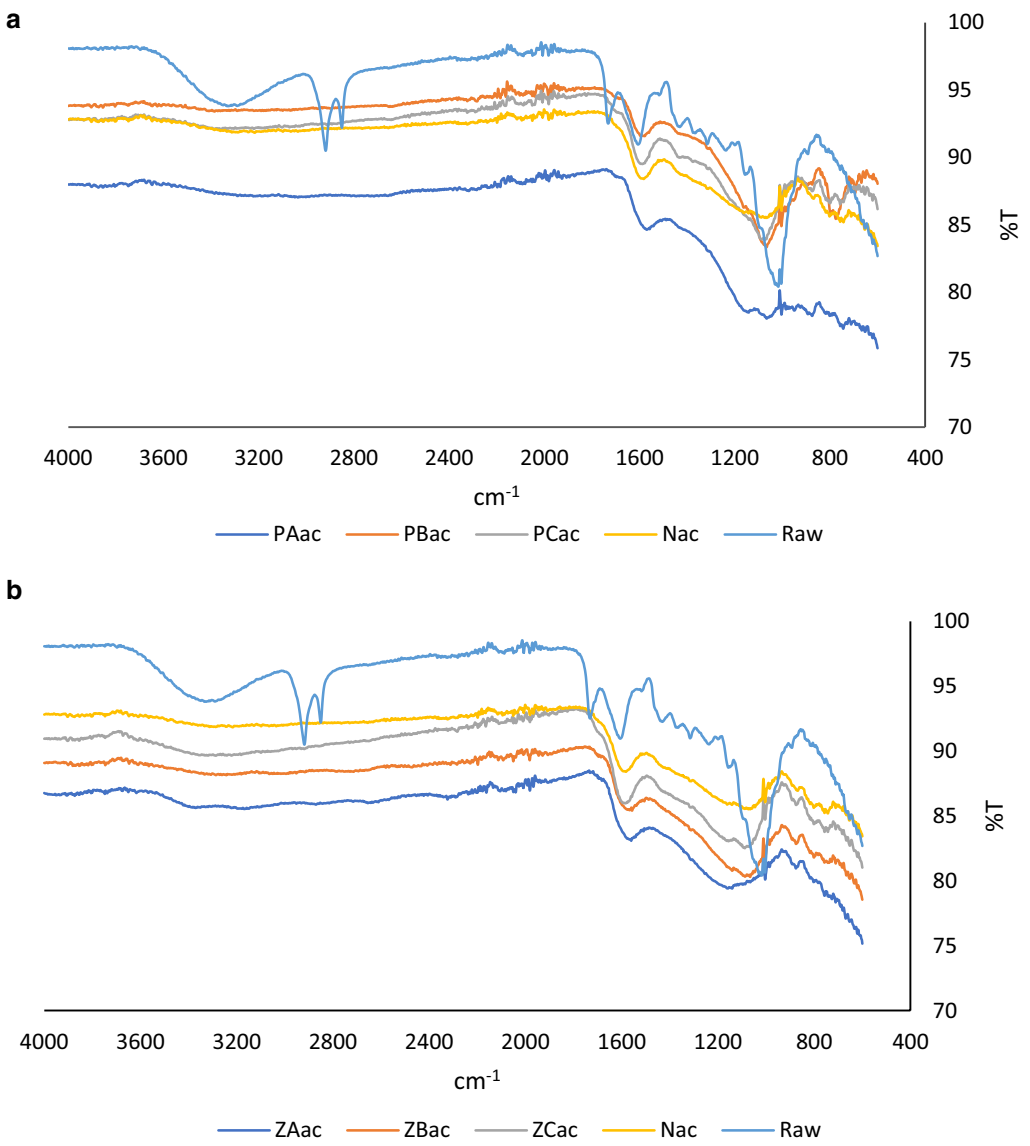

Fig. 2 FTIR spectra of produced chars vs raw biomass **a** H_3PO_4 acid activated and inactivated chars versus raw biomass. **b** $ZnCl_2$ activated and inactivated versus raw biomass. PAac: activated with H_3PO_4 at 5:2 biomass to H_3PO_4 ratio. PBac: activated with H_3PO_4 at 5:1 biomass to H_3PO_4 ratio. PCac: activated with H_3PO_4 at 10:1 biomass to H_3PO_4 ratio. Nac: charred with no activating agent. Raw: raw grape leaf litter. ZAac: activated with $ZnCl_2$ at 5:2 biomass to $ZnCl_2$ ratio. ZBac: activated with $ZnCl_2$ at 5:1 biomass to $ZnCl_2$ ratio. ZCac: activated with $ZnCl_2$ at 10:1 biomass to $ZnCl_2$ ratio

attraction between the adsorbent and adsorbate [52], the higher adsorption observed at pH 3 relative to pH 12 was attributed to this. At high pH, the OH^- ions also competes with adsorbate molecules for adsorption active sites on the activated carbons [26]. Hence, the reduction of phenanthrene adsorption at high pH.

Adsorbent ZAac, performed most efficiently in the removal of phenanthrene from aqueous media comparatively to other adsorbents (Fig. 4). This could be attributed to the surface characteristics of the adsorbent and ionic activities on the sorbent during the adsorption process. Activated carbon with highly microporous structure and improved adsorption capacity were reported to be produced when optimum ratio of $ZnCl_2$ was utilised as activating agent of raw biomass carbonised in an inert atmosphere [53]. This is because, $ZnCl_2$ is a strong dehydrator effective in the removal of hydrogen and oxygen from raw biomass [53].

Effect of adsorbent dosage

Results depicted in Fig. 5 showed that phenanthrene adsorption increased rapidly with increased adsorbent

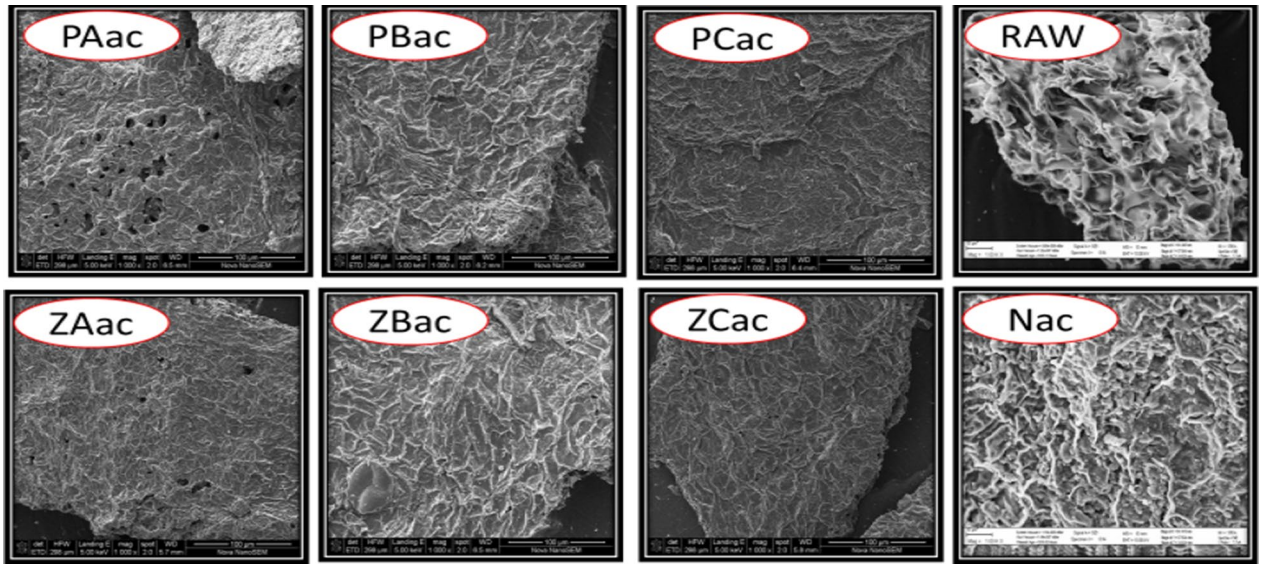

Fig. 3 Scanning electron micrographs of activated carbons, charred and raw biomass (magnification ×1000). PAac: activated with H_3PO_4 at 5:2 biomass to H_3PO_4 ratio. PBac: activated with H_3PO_4 at 5:1 biomass to H_3PO_4 ratio. PCac: activated with H_3PO_4 at 10:1 biomass to H_3PO_4 ratio. Raw: raw grape leaf litter. ZAac: activated with $ZnCl_2$ at 5:2 biomass to $ZnCl_2$ ratio. ZBac: activated with $ZnCl_2$ at 5:1 biomass to $ZnCl_2$ ratio. ZCac: activated with $ZnCl_2$ at 10:1 biomass to $ZnCl_2$ ratio. Nac: charred with no activating agent

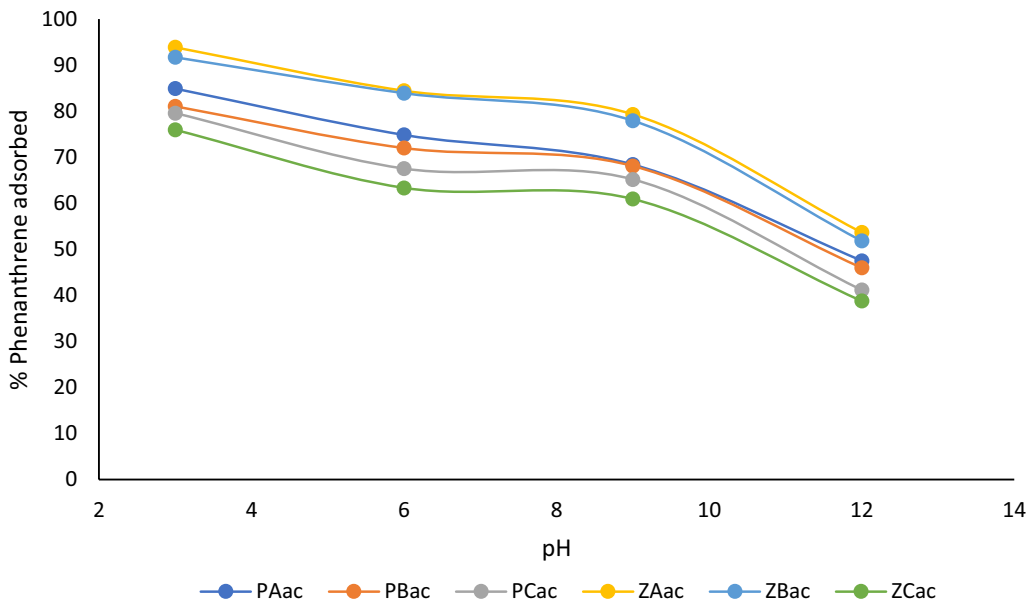

Fig. 4 Effect of aqueous solution pH on phenanthrene removal using activated carbons. Experimental conditions observed: solution concentrations = 1 mg/L, solution volume = 25 mL, adsorbent dosage = 0.1 g, temperature = 298 K, contact time = 180 min and stirring agitation = 100 revolutions per minute (rpm)

dose from 0.01 to 0.05 g, with a gradual increase in adsorption when dose was increased to 0.075 g, while a further increase to 0.1 g of adsorbent dose did not result in a significant increase in adsorption. This observation is consistent with that of Rad et al. [25]. They reported that phenanthrene adsorption increased with the dose of activated carbons until an optimum amount of 0.3 g/100 mL. Up to 8.34 mg/g phenanthrene removal on the activated

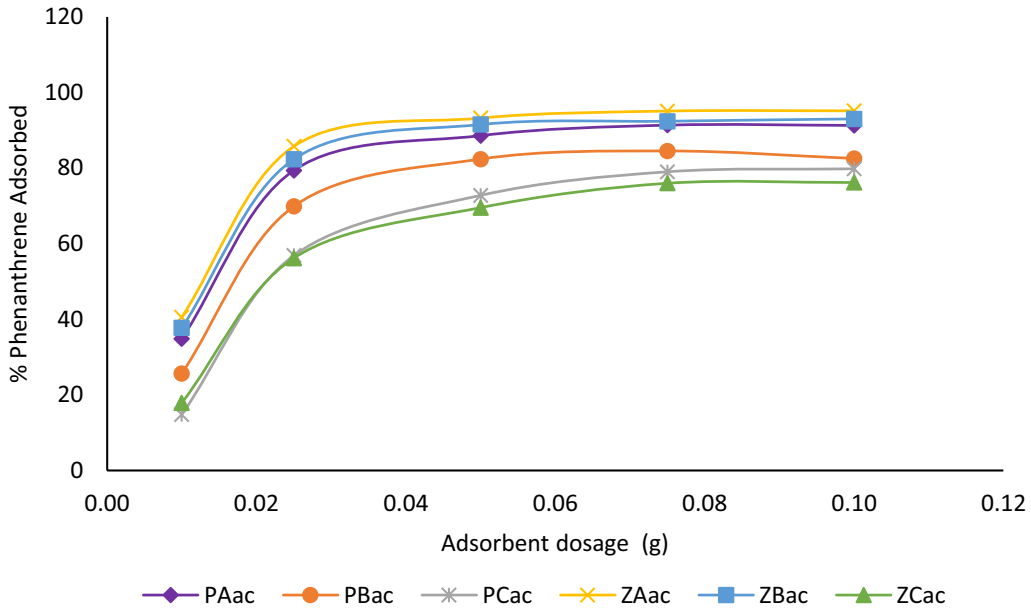

Fig. 5 Effect of adsorbent dosage on phenanthrene removal using activated carbons. Experimental conditions observed: solution concentrations = 1 mg/L, solution volume = 25 mL, pH = 3, temperature = 298 K, contact time = 180 min and stirring agitation = 100 rpm

carbons was achieved. The availability of more sorption active sites with increased adsorbent dose led to the increase in adsorbate removal efficiency at higher adsorbent dosage [54]. The percentage adsorption increased from 59.6 to 99.8% with increased adsorbent dose of 0.2 to 1.0 g/100 mL. In this study, phenanthrene removal of > 90% was obtained with adsorbents PAac, ZAac and ZBac at increased adsorbent dosage.

Effect of initial concentration

Sorption of phenanthrene onto activated carbons at varying initial concentrations of phenanthrene (1 to 5 mg/L) in aqueous solution was studied. Initial phenanthrene concentration of 1 mg/L gave the highest removal efficiency of 92.13% with ZAac (Fig. 6). The percentage of phenanthrene adsorbed decreased with increase in initial adsorbate concentration, although, the concentration of phenanthrene (mg/L) adsorbed increased with increase in initial concentration of phenanthrene. This was due to the availability of more phenanthrene molecules to interact with the active sites of adsorbents. This however did not translate to increased percentage phenanthrene adsorbed, because there was also an increase in the amount of phenanthrene left in solution after the adsorption process. Saturation of adsorption sites on activated carbons surfaces maybe responsible for large percentage of unadsorbed adsorbate molecules [55]. The result obtained is consistent with other studies [54, 56]. The observation of Gupta [26], who carried out batch experiments on the adsorption of phenanthrene in the initial concentration range of 10 to 50 mg/L using 10 mg of activated carbon, is also consistent with the result obtained in this study. Percentage phenanthrene removal from aqueous solution decreased with increase in initial adsorbate concentrations.

Adsorbents ZAac, ZBac and PAac were used for further studies, based on their efficiencies (> 90%) for phenanthrene removal (Fig. 6).

Phenanthrene adsorption isotherms

The Langmuir maximum monolayer coverage capacity (q_m) obtained for phenanthrene adsorption onto adsorbents ZAac, ZBac and PAac were 94.12 mg/g, 60.07 mg/g and 89.13 mg/g, respectively and the corresponding Langmuir isotherm constants (K_L) of 0.48 L/mg, 0.19 L/mg and 0.39 L/mg were obtained, respectively (Table 4). The separation factor R_L values obtained ranged from 0.83 to 0.98. A R_L value of less than one is an indication of favourable equilibrium sorption [29]. Hence, favourable equilibrium sorption of phenanthrene onto the activated carbons were achieved. Coefficient of determination value (R^2) ranged from 0.95 to 0.99, an indication that adsorption data fitted well into Langmuir isotherm model. The data obtained based on Langmuir adsorption isotherm is consistent with that reported by Gupta [26]. A 70.92 mg/g adsorption capacity (q_m) and R^2 value of 0.99 were reported for the adsorption of phenanthrene onto activated carbons produced from orange skin.

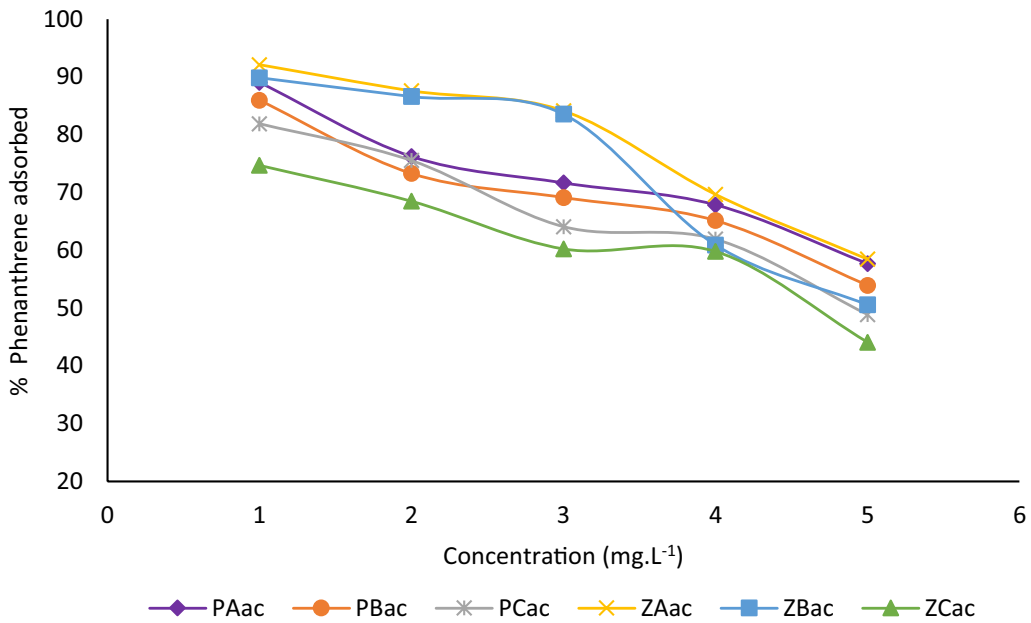

Fig. 6 Effect of initial concentration of phenanthrene on activated carbons' efficiency. Experimental conditions observed: Adsorbent dosage = 0.1 g, solution volume = 25 mL, pH = 3, temperature = 298 K, contact time = 180 min and stirring agitation = 100 rpm

Table 4 Langmuir, Freundlich, Temkin and Dubinin–Radushkevich isotherm constants for the adsorption of phenanthrene onto activated carbons obtained from *V. vinifera*

Isotherm models	Parameters	ZAac	ZBac	PAac
Langmuir	R^2	0.99	0.95	0.98
	q_m (mg/g)	94.12	60.07	89.13
	K_L (L/mg)	0.48	0.19	0.39
	R_L	0.94	0.98	0.83
Freundlich	R^2	0.99	0.97	0.99
	K_f	1.27	1.18	1.16
	1/n	0.75	0.66	0.68
	n	1.33	1.52	1.47
Temkin	R^2	0.94	0.95	0.92
	K_T (L/mg)	0.28	0.26	0.38
	b_T (kJ/mol)	4.03	4.40	3.34
Dubinin–Radushkevich	R^2	0.94	0.92	0.98
	qDRB	2.80	1.13	1.06
	K_{ad} (mol^2/kJ^2)	3.00×10^{-8}	9.00×10^{-9}	4.0×10^{-9}
	E (kJ/mol)	4.08	7.45	11.18

ZAac: activated with $ZnCl_2$ at 5:2 biomass to $ZnCl_2$ ratio, ZBac: activated with $ZnCl_2$ at 5:1 biomass to $ZnCl_2$ ratio, PAac: activated with H_3PO_4 at 5:2 biomass to H_3PO_4 ratio

The data obtained from the Freundlich isotherm modelling showed that experimental data fitted into this isotherm model. The range of 0.97 to 0.99 for R^2 values and K_f range of 1.16 to 1.27 mg/g obtained (Table 4), indicated multilayer loading of phenanthrene on the adsorbents. Moreover, the 1.33 to 1.52 values of n obtained suggested that the adsorption of phenanthrene onto the activated carbons were favourable, this is because the values of n obtained were greater than one but less than ten i.e. $1 < n < 10$ [37]. The data obtained by Rad et al. [25] from the adsorption of phenanthrene with varied initial concentrations (5 to 40 mg/L) using activated carbons (0.3 g to 100 mL) gave R^2 of 0.99, K_f of 2.71 and n of 1.73 based on Freundlich isotherm model. The results they reported were consistent with those obtained in this study. The R^2 values of experimental data obtained from the adsorption process with Freundlich isotherm signified adsorption onto heterogenous surfaces.

The R^2 value range (0.92—0.95) obtained from the Temkin isotherm modelling (Table 4), showed that experimental data fitted considerably well into the Temkin isotherm model, which is an expression of adsorbent–adsorbate interaction, ignoring extremely low and high analytes concentrations [57]. The corresponding 0.26 to 0.38 L/mg and 3.34 to 4.40 kJ/mol ranges were obtained for Temkin isotherm constants K_T, which represents equilibrium binding constant and b_T, which is related to heat of sorption, respectively.

The Dubinin–Radushkevich modelling gave R^2 value range of 0.92 to 0.989. The model was previously utilised to differentiate the physical and chemical adsorption of metal ions [5]. An adsorption mean free energy (E) of

below 8 kJ/mol suggests occurrence of physical adsorption and E values between 8 and 16 kJ/mol suggests the dominance of chemical ion exchange [58]. Hence, the adsorption of phenanthrene onto the $ZnCl_2$ activated carbons ZAac and ZBac with E values of 4.08 and 7.45 kJ/mol, respectively (Table 4) may be considered as physical adsorption. However, the phenanthrene adsorption on the H_3PO_4 activated carbons PAac with E value of 11.18 kJ/mol (Table 4) may be considered to have followed a chemical ion exchange pathway.

The results obtained from isotherm models showed that the adsorption of phenanthrene from aqueous solution onto activated carbons (ZAac, ZBac and PAac), produced from *V. vinifera* leaf litter was favourable. The experimental data fitted best into the Freundlich isotherm model (R^2 of up to 0.999) of the four models employed. This is an indication that heterogenous and multilayer adsorption pathways were dominant in the adsorption of phenanthrene onto the activated carbons. Physical and chemical adsorption processes were responsible for phenanthrene removal. It can be concluded that the activated carbons from *V. vinifera* leaf litter have the potential to serve as biosorbents for the remediation of aqueous solutions and wastewaters contaminated with PAHs.

Adsorption kinetics

Adsorption kinetics study, is crucial in evaluating the efficiency of adsorbents and also in the determination of adsorption mechanism [31]. The effect of contact time on the adsorption of phenanthrene onto activated carbons was studied over time range of 0 to 180 min (Fig. 7). The percentage phenanthrene adsorbed increased with contact time rapidly from 10 to 80 min. After the 80 min contact time, no significant increase in phenanthrene adsorption was recorded, due to dynamic equilibrium being reached. This observation is consistent with that of Gupta [26], who investigated the effect of contact time on phenanthrene adsorption in the time interval of 0 to 150 min. Their study revealed that the amount of phenanthrene adsorbed from aqueous solution onto activated carbons, increased with contact time till 75 min and equilibrium was attained till 150 min.

For the pseudo-first order kinetic model, the value of k_1 was obtained from the slope of the linear plot of $In(q_e - q_t)$ against t. The correlation coefficient (R^2) was also obtained from the linear plot. The value of k_1 obtained for utilizing adsorbents ZAac, ZBac and PAac for phenanthrene adsorption were 3.59 min^{-1}, 2.87 min^{-1}, and 2.34 min^{-1}, respectively (Table 5). The q_e values obtained ranged from 0.46 to 0.73 mg/g and the R^2 value ranged from 0.533 to 0.829. The data therefore did not fit well into pseudo-first order The correlation coefficien model, since the R^2 values obtained were less than < 0.9. The poor fitting of experimental data obtained from the adsorption of phenanthrene onto activated carbons, into pseudo-first order kinetic model had been reported previously [25]. They reported that phenanthrene adsorption showed a better fitting with the pseudo-second order kinetic model relative to the pseudo-first order kinetic model. They concluded that the

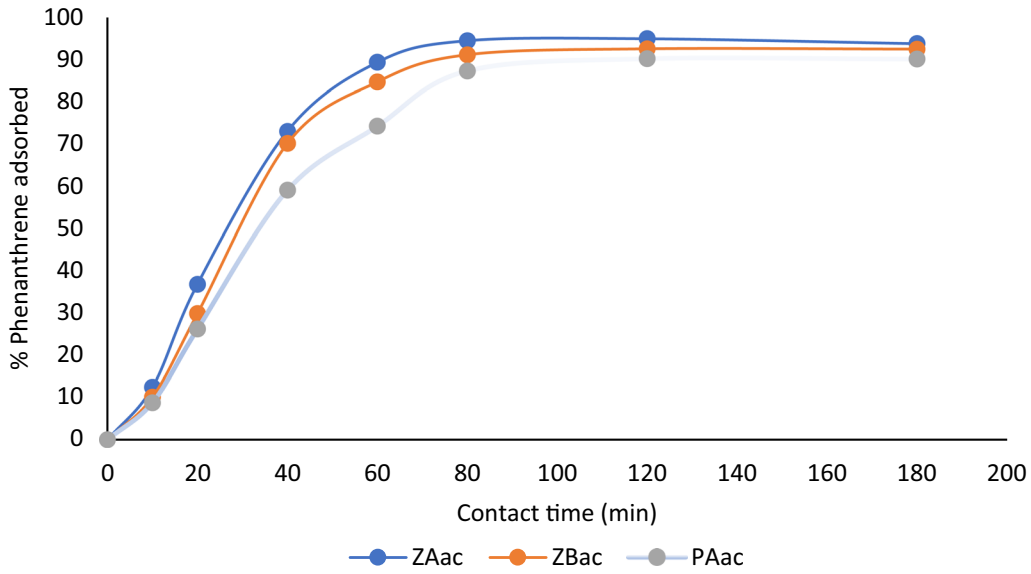

Fig. 7 Effect of contact time on phenanthrene adsorption using activated carbons

Table 5 Adsorption kinetics parameters for the removal of phenanthrene from aqueous solution using activated carbons obtained from *V. vinifera*

Models	Parameters	ZAac	ZBac	PAac
Pseudo first order kinetics	q_e	0.46	0.73	0.70
	K_1(min−1) × 10^{-2}	3.59	2.87	2.34
	R^2	0.82	0.63	0.53
Pseudo second order kinetics	q_e (mg/g)	38.78	50.37	62.58
	K_2 (g (mg/min))	0.76	0.69	0.64
	R^2	0.85	0.75	0.69
Elovich rate equation	α (mg/g min)	0.06	0.05	0.04
	β (g/mg)	3.24	3.16	3.16
	R^2	0.88	0.90	0.94
Intraparticle diffusion	K_{id}	0.09	0.03	0.03
	C	0.08	0.08	0.08
	R^2	0.73	0.75	0.82

ZAac: activated with $ZnCl_2$ at 5:2 biomass to $ZnCl_2$ ratio, ZBac: activated with $ZnCl_2$ at 5:1 biomass to $ZnCl_2$ ratio, PAac: activated with H_3PO_4 at 5:2 biomass to H_3PO_4 ratio

adsorption mechanism of phenanthrene onto activated carbons was predominantly controlled by chemisorption.

The plot of t/q_t against t for the pseudo-second order kinetic model gave a linear relationship, from where q_e and k_2 were determined from the slope and intercept, respectively. The value of k_2 (g (mg/min)) obtained for utilising ZAac, ZBac and PAac were 0.761, 0.692 and 0.637, respectively. The values q_e ranged from 38.78 to 62.58 mg/g with respective R^2 values of 0.696 to 0.8532 (Table 5). The data fitted better into pseudo-second order model relative to pseudo-first order model. This is consistent with the observation of Rad et al. [25].

The α values obtained from the plots of Elovich kinetic model ranged from 0.04 to 0.06 mg/g min, while the β values ranged from 3.16 to 3.24 g/mg and the respective R^2 range of 0.88 to 0.94 was obtained (Table 5). The range of β obtained in this study is an indication that the adsorbed phenanthrene molecules onto activated carbons were sufficiently held and may not be easily desorbed.

A straight-line graph would be obtained from the Weber Morris intraparticle diffusion kinetic model plots (plot of q_t vs $t^{1/2}$) when the sorption process is controlled by intraparticle diffusion only. However, if multi-linear plots were obtained, then it suggests that two or more steps (such as film diffusion and equilibrium adsorption) affected the sorption process [40]. The plots of q_t vs $t^{1/2}$ obtained from this study could be divided into a sharp rise (step 1) and flat portion (step 2) as shown in Fig. 8. Hence, the sorption processes of phenanthrene onto activated carbons (ZAac, ZBac and PAac) were affected by two or more steps. The values of K_{id}, C, and R^2 Weber Morris intraparticle diffusion model parameters are presented in Table 5.

Based on the R^2 values obtained from the kinetic study, experimental data fitted best into the Elovich kinetic model relative to other kinetic models (Table 5). Hence,

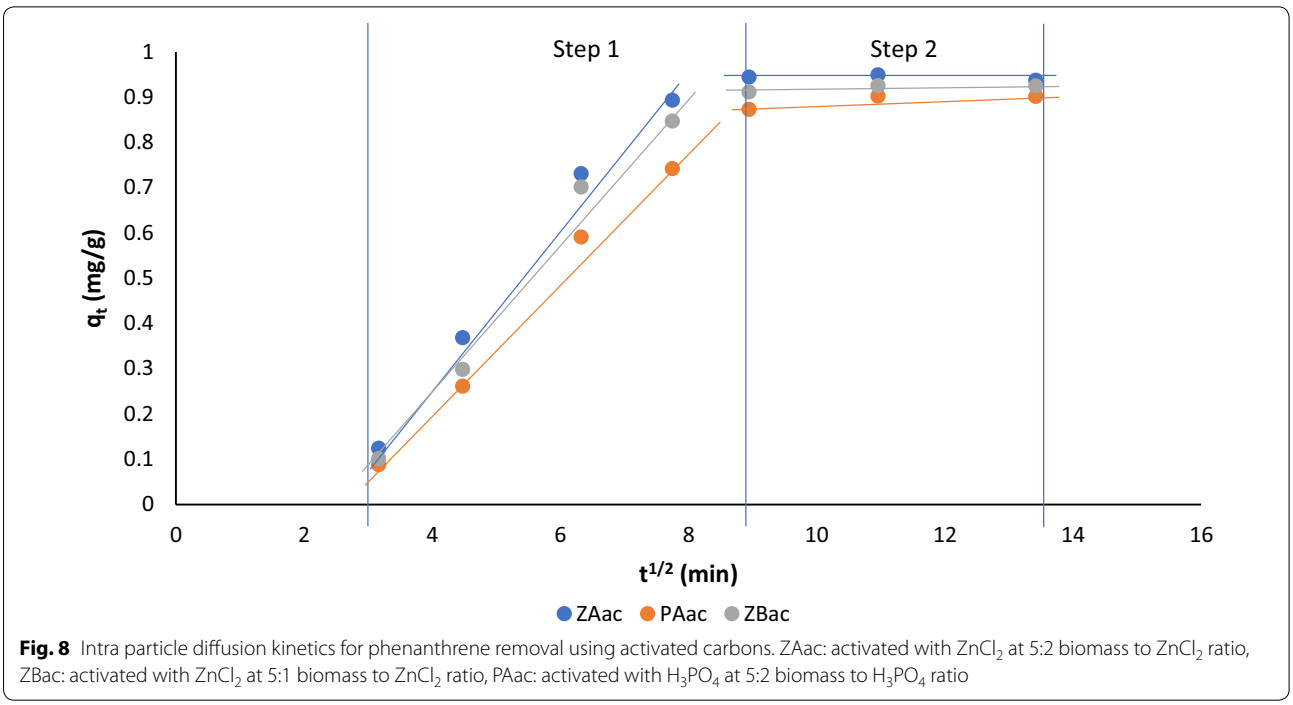

Fig. 8 Intra particle diffusion kinetics for phenanthrene removal using activated carbons. ZAac: activated with $ZnCl_2$ at 5:2 biomass to $ZnCl_2$ ratio, ZBac: activated with $ZnCl_2$ at 5:1 biomass to $ZnCl_2$ ratio, PAac: activated with H_3PO_4 at 5:2 biomass to H_3PO_4 ratio

chemisorption was deduced as a major phenanthrene removal pathway from aqueous solution.

The SEM images of these adsorbents before and after they were utilised for phenanthrene adsorption showed significant changes in surface texture (Fig. 9). The SEM images of activated carbons after phenanthrene adsorption had significantly smoother surface morphology, which could be attributed to accumulation of phenanthrene onto the adsorbent's surfaces.

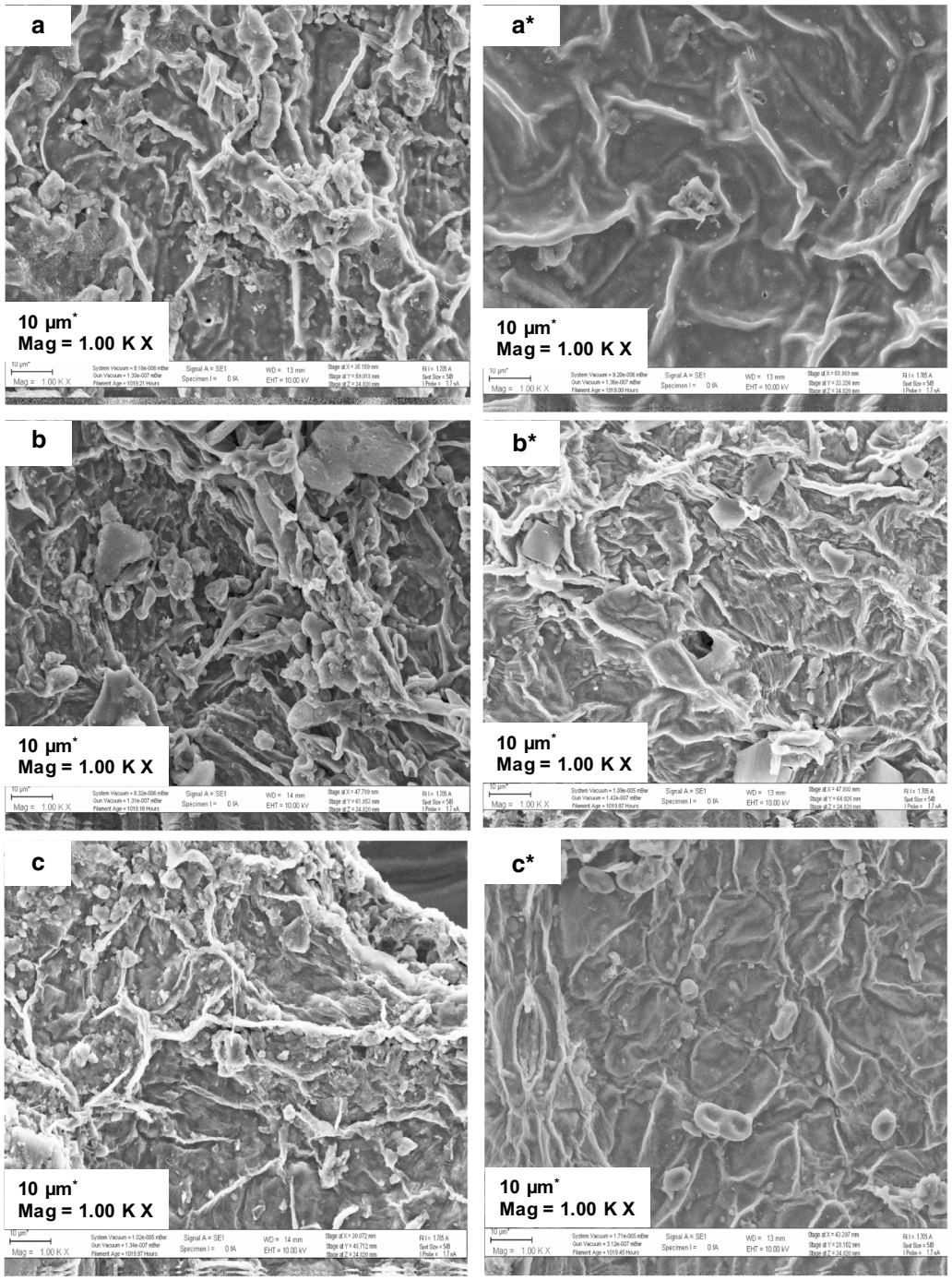

Fig. 9 SEM images of activated carbons before and after adsorption of phenanthrene from aqueous solution. **a** ZAac (activated with $ZnCl_2$ at 5:2 biomass to $ZnCl_2$ ratio). **b** ZBac (activated with $ZnCl_2$ at 5:1 biomass to $ZnCl_2$ ratio). **c** PAac (activated with H_3PO_4 at 5:2 biomass to H_3PO_4 ratio)

Acknowledgements
Prof. B.O. Opeolu. acknowledges the National Research Foundation (NRF), South Africa, through the Thuthuka Research Grant No. 84185. The authors thank Dr B.O Fagbayigbo for his technical assistance.

Authors' contributions
AAA planned the experiments and drafted the manuscript, while OSA assisted with the writing and modelling. OSF, VAJ and RS contributed materials and editorials, while BOO, supervised the study and revised the manuscript. All authors read and approved the final manuscript.

Funding
National Research Foundation (NRF), South Africa, through the Thuthuka Research Grant No. 84185, funded this project.

Availability of data and materials
Datasets used and/or analysed during the current study that are not included in the manuscript are available from the corresponding author on reasonable request.

Competing interests
The authors declare that they have no competing interests.

Author details
[1] Department of Chemistry, Cape Peninsula University of Technology, Cape Town, South Africa. [2] Department of Environmental and Occupational Studies, Faculty of Applied Sciences, Cape Peninsula University of Technology, Cape Town, South Africa. [3] Faculty of Applied Sciences, Cape Peninsula University of Technology, Cape Town, South Africa. [4] Department of Industrial Chemistry, Federal University Oye Ekiti, Oye Ekiti, Nigeria. [5] Department of Biotechnology and Consumer Science, Cape Peninsula University of Technology, Cape Town, South Africa. [6] Department of Conservation and Marine Sciences, Cape Peninsula University of Technology, Cape Town, South Africa.

Received: 3 December 2019 Accepted: 31 January 2020
Published online: 14 February 2020

References

1. Kennish MJ (2002) Environmental threats and environmental future of estuaries. Environ Conserv 29:78–107
2. Moore MN, Depledge MH, Readman JW, Paul Leonard DR (2004) An integrated biomarker-based strategy for ecotoxicological evaluation of risk in environmental management. Mutat Res 552:247–268
3. Sumpter JP (2009) Protecting aquatic organisms from chemicals: the harsh realities. Philos Trans R Soc A 367:3877–3894
4. Dailianis S, Tsarpali V, Melas K, Karapanagioti HK, Manariotis ID (2014) Aqueous phenanthrene toxicity after high-frequency ultrasound degradation. Aquat Toxicol 147:32–40
5. Foo KY, Hameed BH (2010) Insights into the modeling of adsorption isotherm systems. Chem Eng J 156(1):2–10
6. Munir MT, Li B, Boiarkina I, Baroutian S, Yu W, Young BR (2017) Phosphate recovery from hydrothermally treated sewage sludge using struvite precipitation. Bioresour Technol 239:171–179
7. Sarasidis VC, Plakas KV, Karabelas AJ (2017) Novel water-purification hybrid processes involving in-situ regenerated activated carbon, membrane separation and advanced oxidation. Chem Eng J 328:1153–1163
8. Shattar SFA, Zakaria NA, Foo KY (2016) Feasibility of montmorillonite-assisted adsorption process for the effective treatment of organo-pesticides. Desalin Water Treat 57:13645–13677
9. Demirbas E, Kobya M, Senturk E, Ozkan T (2004) Adsorption kinetics for the removal of chromium (VI) from aqueous solutions on the activated carbons prepared from agricultural wastes. Water SA 30:533–539
10. Ioannidou O, Zabaniotou A (2007) Agricultural residues as precursors for activated carbon production: a review. Renew Sustain Energy Rev 11(9):1966–2005
11. Ho Y-S, Chiang T-H, Hsueh Y-M (2005) Removal of basic dye from aqueous solution using tree fern as a biosorbent. Process Biochem 40(1):119–124
12. Aksu Z (2005) Application of biosorption for the removal of organic pollutants: a review. Process Biochem 40(3):997–1026
13. Chen B, Yuan M, Liu H (2011) Removal of polycyclic aromatic hydrocarbons from aqueous solution using plant residue materials as a biosorbent. J Hazard Mater 188:436–442
14. Li Y, Chen B, Zhu L (2010) Enhanced sorption of polycyclic aromatic hydrocarbons from aqueous solution by modified pine bark. Bioresour Technol 101:7307–7313
15. Saeed A, Sharif M, Iqbal M (2010) Application potential of grapefruit peel as dye sorbent: kinetics, equilibrium and mechanism of crystal violet adsorption. J Hazard Mater 179(1):564–572
16. Chand R, Narimura K, Kawakita H, Ohto K, Watari T, Inoue K (2009) Grape waste as a biosorbent for removing Cr(VI) from aqueous solution. J Hazard Mater 163(1):245–250
17. Spinelli R, Nati C, Pari L, Mescalchin E, Magagnotti N (2012) Production and quality of biomass fuels from mechanized collection and processing of vineyard pruning residues. Appl Energy 89(1):374–379
18. Lafka T-I, Sinanoglou V, Lazos ES (2007) On the extraction and antioxidant activity of phenolic compounds from winery wastes. Food Chem 104(3):1206–1214
19. Siphugu L, Terry L. South Africa—Republic of wine annual. Pretoria, South Africa. 2011. https://gain.fas.usda.gov/RecentGAINPublications/WineAnnual_Pretoria_SouthAfrica-Republicof_3-14-2011.pdf. Accessed 20 Jan 2018
20. Wang X, Qin Y (2005) Equilibrium sorption isotherms for of Cu^{2+} on rice bran. Process Biochem 40(2):677–680
21. Garg UK, Kaur MP, Garg VK, Sud D (2007) Removal of hexavalent chromium from aqueous solution by agricultural waste biomass. J Hazard Mater 140(1):60–68
22. Opeolu BO, Bamgbose O, Fatoki OS (2011) Zinc abatement from simulated and industrial wastewaters using sugarcane biomass. Water SA 37(3):313–320
23. Sudaryanto Y, Hartono SB, Irawaty W, Hindarso H, Ismadji S (2006) High surface area activated carbon prepared from cassava peel by chemical activation. Bioresour Technol 97:734–739
24. Darmawan S, Wistara NJ, Pari G, Maddu A, Syafii W (2016) Characterisation of lignocellulosic biomass as raw material for the production of porous carbon-based materials. BioResources 11(2):3561–3574
25. Rad RM, Omidi L, Kakooei H, Golbabaei F, Hassani H, Loo RA et al (2014) Adsorption of polycyclic aromatic hydrocarbons on activated carbons: kinetic and isotherm curve modeling. Int J Occup Hyg 6:43–49
26. Gupta H (2015) Removal of phenanthrene from water using activated carbon developed from orange rind. Int J Sci Res Environmetal Sci 3(7):248–255
27. Tiwari JN, Mahesh K, Le NH, Kemp KC, Timilsina R, Tiwari RN et al (2013) Reduced graphene oxide-based hydrogels for the efficient capture of dye pollutants from aqueous solutions. Carbon 56:173–182
28. Weber TW, Chakravorti RK (1974) Pore and solid diffusion models for fixed-bed adsorbers. Am Inst Chem Eng J 20(2):228–238
29. El Qada EN, Allen SJ, Walker GM (2006) Adsorption of methylene blue onto activated carbon produced from steam activated bituminous coal: a study of equilibrium adsorption isotherm. Chem Eng J 124(1–3):103–110
30. Walker GM, Weatherley LR (2001) Adsorption of dyes from aqueous solution—the effect of adsorbent pore size distribution and dye aggregation. Chem Eng J 83(3):201–206
31. Aljeboree AM, Alshirifi AN, Alkaim AF (2017) Kinetics and equilibrium study for the adsorption of textile dyes on coconut shell activated carbon. Arab J Chem 10:S3381–S3393
32. Rahim AA, Garba ZN (2016) Efficient adsorption of 4-Chloroguiacol from aqueous solution using optimal activated carbon: equilibrium isotherms and kinetics modeling. J Assoc Arab Univ Basic Appl Sci 21:17–23
33. Nguyen C, Do DD (2001) The Dubinin–Radushkevich equation and the underlying microscopic adsorption description. Carbon N Y 39:1327–1336
34. Dada A, Olalekan A, Olatunya A, Dada O (2012) Langmuir, Freundlich, Temkin and Dubinin–Radushkevich isotherms studies of equilibrium sorption of Zn^{2+} onto phosphoric acid modified rice husk. IOSR J Appl Chem 3(1):38–45

35. Sun Y, Li H, Li G, Gao B, Yue Q, Li X (2016) Characterisation and ciprofloxacin adsorption properties of activated carbons prepared from biomass wastes by H_3PO_4 activation. Bioresour Technol 217:239–244
36. Ho YS, McKay G (1999) Pseudo-second order model for sorption processes. Process Biochem 34(5):451–465
37. Sarada B, Prasad MK, Kumar KK, Ramachandra Murthy CV (2014) Cadmium removal by macro algae *Caulerpa fastigiata*: characterization, kinetic, isotherm and thermodynamic studies. J Environ Chem Eng 2(3):1533–1542
38. Ho YS, McKay G (1998) A comparison of chemisorption kinetic models applied to pollutant removal on various sorbents. Process Saf Environ Prot 76(4):332–340
39. Wu F-C, Tseng R-L, Juang R-S (2009) Characteristics of Elovich equation used for the analysis of adsorption kinetics in dye-chitosan systems. Chem Eng J 150(2–3):366–373
40. Fierro V, Torné-Fernández V, Montané D, Celzard A (2008) Adsorption of phenol onto activated carbons having different textural and surface properties. Microporous Mesoporous Mater 111(1–3):276–284
41. Asuquo ED, Martin AD (2016) Sorption of cadmium (II) ion from aqueous solution onto sweet potato (*Ipomoea batatas* L.) peel adsorbent: characterisation, kinetic and isotherm studies. J Environ Chem Eng 4(4):4207–4228
42. Adebowale KO, Bayer E (2002) Active carbons from low temperature conversion chars. https://inis.iaea.org/search/search.aspx?orig_q=RN:33050383. Accessed 8 May 2017.
43. Rashidi NA, Yusup S, Ahmad MM, Mohamed NM, Hameed BH (2012) Activated carbon from the renewable agricultural residues using single step physical activation: a preliminary analysis. APCBEE Procedia 3:84–92
44. Molina-Sabio M, Rodríguez-Reinoso F (2004) Role of chemical activation in the development of carbon porosity. Colloids Surf A Physicochem Eng Asp 241(1–3):15–25
45. Sugumaran P, Susan VP, Ravichandran P, Seshadri S (2012) Production and characterisation of activated carbon from banana empty fruit bunch and *Delonix regia* fruit pod. J Sustain Energy Environ 3:125–132
46. Prahas D, Kartika Y, Indraswati N, Ismadji S (2008) Activated carbon from jackfruit peel waste by H3PO4 chemical activation : pore structure and surface chemistry characterization. Chem Eng J 140:32–42
47. Bagheri N, Abedi J (2009) Preparation of high surface area activated carbon from corn by chemical activation using potassium hydroxide. Chem Eng Res Des 87(8):1059–1064
48. Correa RC, Otto T, Kruse A (2017) Influence of the biomass components on the pore formation of activated carbon. Biomass Bioenerg 97:53–64
49. Lawal IA, Chetty D, Akpotu SO, Moodley B (2017) Sorption of Congo red and reactive blue on biomass and activated carbon derived from biomass modified by ionic liquid. Environ Nanotechnol Monit Manag 8:83–91
50. Dodevski V, Jankovi B, Stojmenovi M, Krsti S, Popovi J, Pagnacco MC et al (2017) Plane tree seed biomass used for preparation of activated carbons (AC) derived from pyrolysis Modeling the activation process. Colloids Surf A Physicochem Eng Asp 522:83–96
51. Deng J, Xiong T, Wang H, Zheng A, Wang Y (2016) Effects of cellulose, hemicellulose, and lignin on the structure and morphology of porous carbons. ACS Sustain Chem Eng 4:3750–3756
52. Özcan AS, Erdem B, Özcan A (2004) Adsorption of acid blue 193 from aqueous solutions onto Na–bentonite and DTMA–bentonite. J Colloid Interface Sci 280(1):44–54
53. Kim JW, Sohn MH, Kim DS, Sohn SM, Kwon YS (2001) Production of granular activated carbon from waste walnut shell and its adsorption characteristics for Cu^{2+} ion. J Hazard Mater 85(3):301–315
54. Garg V, Gupta R, Bala Yadav A, Kumar R (2003) Dye removal from aqueous solution by adsorption on treated sawdust. Bioresour Technol 89(2):121–124
55. Qiao K, Tian W, Bai J, Dong J, Zhao J, Gong X et al (2018) Preparation of biochar from *Enteromorpha prolifera* and its use for the removal of polycyclic aromatic hydrocarbons (PAHs) from aqueous solution. Ecotoxicol Environ Saf 149:80–87
56. Lamichhane S, Bal Krishna KC, Sarukkalige R (2016) Polycyclic aromatic hydrocarbons (PAHs) removal by sorption: a review. Chemosphere 148:336–353
57. Qu Y, Zhang C, Li F, Bo X, Liu G, Zhou Q (2009) Equilibrium and kinetics study on the adsorption of perfluorooctanoic acid from aqueous solution onto powdered activated carbon. J Hazard Mater 169:146–152
58. Akar T, Celik S, Akar ST (2010) Biosorption performance of surface modified biomass obtained from *Pyracantha coccinea* for the decolorisation of dye contaminated solutions. Chem Eng J 160(2):466–472

Publisher's Note